Sulfenic Acid Formation in Human Serum Albumin by Hydrogen Peroxide and Peroxynitrite

6 **AUTHORS**, INCLUDING:

Rafael Radi
University of the Republic, Uruguay
311 PUBLICATIONS **22,641** CITATIONS

SEE PROFILE

Stepehn Barnes
University of Alabama at Birmingham
344 PUBLICATIONS **16,171** CITATIONS

SEE PROFILE

Bruce A Freeman
University of Pittsburgh
350 PUBLICATIONS **37,361** CITATIONS

SEE PROFILE

Sulfenic Acid Formation in Human Serum Albumin by Hydrogen Peroxide and Peroxynitrite[†]

Sebastián Carballal,[‡,§] Rafael Radi,[§] Marion C. Kirk,[ǁ] Stephen Barnes,[ǁ,⊥, #] Bruce A. Freeman,[⊥,¶] and Beatriz Alvarez*,[‡]

Laboratorio de Enzimología, Facultad de Ciencias y Departamento de Bioquímica, Facultad de Medicina,
Universidad de la República, Montevideo, Uruguay, Departments of Anesthesiology, Biochemistry and Molecular Genetics,
Pharmacology and Toxicology, Cancer Center Mass Spectrometry Shared Facility and Center for Free Radical Biology,
University of Alabama at Birmingham, Birmingham, Alabama 35294

ABSTRACT: Human serum albumin (HSA), the most abundant protein in plasma, has been proposed to have an antioxidant role. The main feature responsible for this property is its only thiol, Cys34, which comprises ~80% of the total free thiols in plasma and reacts preferentially with reactive oxygen and nitrogen species. Herein, we show that the thiol in HSA reacted with hydrogen peroxide with a second-order rate constant of 2.26 M^{-1} s^{-1} at pH 7.4 and 37 °C and a 1:1 stoichiometry. The formation of intermolecular disulfide dimers was not observed, suggesting that the thiol was being oxidized beyond the disulfide. With the reagent 7-chloro-4-nitrobenzo-2-oxa-1,3-diazol (NBD-Cl), we were able to detect the formation of sulfenic acid (HSA-SOH) from the UV–vis spectra of its adduct. The formation of sulfenic acid in Cys34 was confirmed by mass spectrometry using 5,5-dimethyl-1,3-cyclohexanedione (dimedone). Sulfenic acid was also formed from exposure of HSA to peroxynitrite, the product of the reaction between nitric oxide and superoxide radicals, in the absence or in the presence of carbon dioxide. The latter suggests that sulfenic acid can also be formed through free radical pathways since following reaction with carbon dioxide, peroxynitrite yields carbonate radical anion and nitrogen dioxide. Sulfenic acid in HSA was remarkably stable, with ~15% decaying after 2 h at 37 °C under aerobic conditions. The formation of glutathione disulfide and mixed HSA-glutathione disulfide was determined upon reaction of hydrogen peroxide-treated HSA with glutathione. Thus, HSA-SOH is proposed to serve as an intermediate in the formation of low molecular weight disulfides, which are the predominant plasma form of low molecular weight thiols, and in the formation of mixed HSA disulfides, which are present in ~25% of circulating HSA.

Human serum albumin (HSA)[1] is the most abundant protein in plasma, present at a concentration of ~0.6 mM. In a total of 585 amino acids, this globular 66 kDa protein contains 18 tyrosines, six methionines, one tryptophan, 17 disulfide bridges, and only one free cysteine, Cys34. The functions of HSA include the maintenance of colloid osmotic pressure and the binding and transport of several ligands (i.e., fatty acids, hormones). Albumin is also proposed to serve an antioxidant function in the vascular compartment because of its scavenging of reactive oxygen and nitrogen species that are generated by basal aerobic metabolism and can be produced at increased rates during inflammation (*1*, *2*).

The main substituent responsible for the antioxidant properties of HSA is the thiol in Cys34, which accounts for ~80% of net free thiols in plasma. Our previous work has shown that, in contrast to lipids and other biomolecules, HSA-SH is the preferential plasma scavenger of reactive species derived from the enzyme xanthine oxidase, the products of which include hydrogen peroxide, superoxide, and hydroxyl radical (*3*). Furthermore, the thiol residue of HSA reacts preferentially with peroxynitrite, the product of the reaction between nitric oxide and superoxide radicals, leading to thiol oxidation (*4*, *5*). HSA-SH has also been shown to react with phospholipid hydroperoxides (*6*). The importance of HSA-SH as a scavenger of reactive species is inferred by the observation that the thiol content of HSA

* To whom correspondence should be addressed. Laboratorio de Enzimología, Facultad de Ciencias, Iguá 4225, 11400 Montevideo, Uruguay. Fax: 5982 5250749. E-mail: Beatriz.Alvarez@fcien.edu.uy.
[‡] Laboratorio de Enzimología, Facultad de Ciencias.
[§] Departamento de Bioquímica, Facultad de Medicina.
[ǁ] Cancer Center Mass Spectrometry Shared Facility, UAB.
[⊥] Biochemistry and Molecular Genetics, UAB.
[#] Pharmacology and Toxicology, UAB.
[¶] Anesthesiology and Center for Free Radical Biology, UAB.
[1] Abbreviations: HSA, human serum albumin; HSA-SH, the thiol of HSA; BSA, bovine serum albumin; SH/HSA, amount of thiol per albumin molecule; DTPA, diethylenetriaminepentaacetic acid; EDTA, ethylenediaminetetraacetic acid; NBD-Cl, 7-chloro-4-nitrobenzo-2-oxa-1,3-diazol; DTNB, 5,5′-dithio-bis(2-nitrobenzoic acid); dimedone, 5,5-dimethyl-1,3-cyclohexanedione; GSH, glutathione; GSSG, glutathione disulfide; SDS–PAGE, sodium dodecyl sulphate polyacrylamide gel electrophoresis.

(SH/HSA) decreases with aging, from 0.7−0.76 SH/HSA in young subjects to 0.48−0.56 in the 60−89 year old range (*7, 8*). In addition, HSA supplementation of septic patients significantly elevates plasma thiol content (*9*), suggesting possible benefits of HSA in vascular defenses against reactive inflammatory mediators.

Freshly isolated HSA is heterogeneous with respect to its thiol content, reported as typically 0.6−0.7 SH/HSA (*10*). The main HSA fraction is called mercaptalbumin and contains the free thiol. The other fraction, nonmercaptalbumin, contains a high percentage of mixed disulfides between Cys34 and cysteine or other low molecular weight thiols. The rest of the plasma nonmercaptalbumin fraction is not reducible with reagents such as dithiothreitol, and in this fraction the thiol is oxidized to higher oxidation states including sulfinic and sulfonic acids (*11*). A small amount of dimers and higher oligomers that increase with purification and storage can also be observed. In turn, low molecular weight thiols circulate predominantly as disulfides, either bound to protein or to other low molecular weight thiols.

The two-electron oxidation of a thiol (RSH) yields sulfenic acid (RSOH). In contrast to the disulfide (RSSR), or sulfinic (RSO_2H) and sulfonic acids (RSO_3H), sulfenic acid is typically unstable and highly reactive. Sulfenic acids exhibit nucleophilic reactivity, and the sulfur can be the target of nucleophilic attack as well. Thus, a sulfenic acid can react with another thiol yielding disulfides or condense with a second sulfenic acid, forming thiosulfinates (*12*).

The biological formation of sulfenic acid is receiving renewed interest. Sulfenic acids have been detected in a number of proteins and enzymes, where they are proposed to serve catalytic and signaling functions (for review, see refs *12* and *13*). For sulfenic acid to be stabilized in a protein, the absence of thiols close to the site of formation is required, as well as adequate hydrogen bonding partners and/or stabilization of the corresponding sulfenate, together with limited solvent access such as is present in an apolar microenvironment.

In this report, we reveal and characterize the formation of a stable sulfenic acid in HSA following its reaction with hydrogen peroxide and peroxynitrite and propose a role for this key intermediate of HSA oxidation in the formation of mixed HSA disulfides and low molecular weight disulfides.

EXPERIMENTAL PROCEDURES

Materials. HSA (USP) was from Baxter Healthcare (Glendale, CA), catalase was from Fluka, hydrogen peroxide was from Baker, trypsin (modified sequencing grade) was from Roche, and the remaining reagents were from Sigma Aldrich.

Solutions. HSA was delipidated with activated charcoal (*14*) and incubated overnight with 2-mercaptoethanol (10 mM) at 4 °C, followed by gel filtration on Sephadex G-25 against phosphate buffer (20 mM, pH 7.4, DTPA 0.1 mM). HSA solutions thus prepared had a concentration of ∼1 mM and typically 0.6−0.9 SH/HSA. The concentration of HSA solutions was determined from absorbance at 279 nm ($\epsilon =$ 0.531 $(g/L)^{-1}$ cm^{-1}), assuming a molecular weight of 66 486 (*15*). Hydrogen peroxide solutions were prepared in Nanopure water, and their concentration was determined from absorbance at 240 nm ($\epsilon = 43.6$ M^{-1} cm^{-1}, (*16*)). Peroxynitrite was synthesized from hydrogen peroxide and nitrite

in a quenched flow reactor (*17, 18*). Excess hydrogen peroxide was removed with manganese dioxide. The concentration of peroxynitrite solutions was determined from absorbance at 302 nm ($\epsilon = 1670$ M^{-1} cm^{-1}, (*19*)), and nitrite content was less than 0.3 nitrite per peroxynitrite. 7-Chloro-4-nitrobenzo-2-oxa-1,3-diazol (NBD-Cl) and 5,5-dimethyl-1,3-cyclohexanedione (dimedone) solutions were prepared in dimethyl sulfoxide and 95% ethanol, respectively. Cysteine solutions were prepared in water under anaerobic conditions. Cystine was prepared in 0.1 M sodium hydroxide. Unless specified, all assays were performed in fresh phosphate buffer, pH 7.4, containing DTPA (0.1 mM) at 37 °C. When sodium bicarbonate (25 mM) was included, the initial pH of the buffer was lowered so that after bicarbonate addition the final pH was 7.4. The amount of carbon dioxide present (1.2 mM) was calculated according to a pK_a of 6.1 for the pair carbon dioxide/bicarbonate.

Thiol and Nitrotyrosine Determinations. Thiols were determined with 5,5′-dithiobis-(2-nitrobenzoic acid) (DTNB), after incubating HSA with an excess of DTNB in sodium pyrophosphate buffer (0.1 M, pH 9) for 25 min in the dark, at room temperature. An absorption coefficient at 412 nm of 13.6 mM^{-1} cm^{-1} (*20*) was used to quantify the 5-thio-3-nitrobenzoate anion, with the absorbance of the DTNB solution and the intrinsic low absorbance of HSA at this wavelength accounted for. Nitrotyrosine formation in HSA was determined from the increase in absorbance at 430 nm ($\epsilon = 4.3$ mM^{-1} cm^{-1}, (*21*)) after alkalinization of the samples to pH ≥ 10 with sodium hydroxide (5 N, less than 1% of the total volume).

Kinetics and Stoichiometry of the Reaction between Hydrogen Peroxide and the Thiol in HSA. The rate constant of the reaction between hydrogen peroxide and HSA-SH was determined using pseudo-first-order conditions. Reactions were started by the addition of increasing concentrations of hydrogen peroxide (1.55−4.42 mM) to HSA (0.25 mM). At different time points, aliquots were removed, catalase (100 U mL^{-1}) was added, and samples were immediately assayed for thiol content. The results were fitted to a single-exponential function to determine the pseudo-first-order rate constants. To determine the stoichiometry, a similar experiment was performed with 0.5 mM HSA and 0−0.5 mM hydrogen peroxide, with thiols quantified after the reaction was complete (75 min).

SDS−PAGE. Electrophoresis was performed in 10% polyacrylamide gels containing sodium dodecyl sulfate. The samples were prepared under reducing and nonreducing conditions, depending on the presence of 2-mercaptoethanol in the sample buffer. Proteins were visualized with Coomassie Blue.

Trapping of Sulfenic Acid with NBD-Cl. HSA (0.5 mM) was exposed to oxidants (0.4 mM) for 30 or 5 min, respectively, for hydrogen peroxide and peroxynitrite or peroxynitrite/CO_2. NBD-Cl (1 mM) was added to the samples and subjected to gel filtration 30 min later on PD-10 columns (Pharmacia) equilibrated with phosphate buffer (20 mM, pH 7.4, DTPA 0.1 mM). Spectra were recorded in a Shimadzu UV-1603 spectrophotometer, and HSA concentration was determined at 279 nm, a measurement giving results similar to the Biuret reaction. Spectra were also obtained for low molecular weight thiols under different oxidation states (L-cysteic acid, L-cysteine sulfinic acid, cysteine, GSH, and

cystine) by mixing 0.1 mM compounds with 0.1 mM NBD-Cl.

Trapping of Sulfenic Acid with Dimedone and Mass Spectrometry. HSA (0.5 mM) was exposed to hydrogen peroxide (1 mM) for 30 min. Dimedone (2.5 mM) was added, and after 30 min agitation at room temperature, the protein was passed through a water-equilibrated gel filtration column. To 1 mg (~30 μL) of control or hydrogen peroxide-treated HSA, 200 μL of Tris buffer (0.2 M, pH 8) containing 6 M guanidine hydrochloride was added. The samples were purged with argon and incubated for 2 h at 37 °C. Then, the thiols were reduced overnight with dithiothreitol (60 mM) and carboxymethylated with iodoacetic acid (216 mM) for 1 h in the dark at room temperature, followed by the addition of 2-mercaptoethanol (248 mM). The samples were washed and concentrated by ultrafiltration and resuspended in 200 μL of ammonium bicarbonate (0.1 M). Trypsin (10 μg) was added and left overnight at 37 °C. Peptide fragments were separated on a reverse phase HPLC column (300 μM ID × 15 cm C18 PepMap) at a flow rate of 2 μL min^{-1} with a gradient from 20 to 100% acetonitrile/0.1% formic acid over a period of 20 min. Electrospray mass spectrometry was performed on a Q-TOF III MS (Micromass, Manchester, UK) with automatic functional switching between survey MS and MS-MS modes. A multiply charged peak above 6 counts detected in the mass spectrum was automatically selected for tandem MS analysis.

Reaction of Sulfenic Acid with GSH and Formation of Disulfides. HSA (0.5 mM) was preincubated with hydrogen peroxide (5 mM) for 5 min at 37 °C. After stopping the reactions with catalase (200 U mL^{-1}), aliquots (1 mL) were taken at various times, added directly to GSH (0.4 mM), and incubated for 30 min at 37 °C. Then, HSA was precipitated with perchloric acid (0.4 M) and centrifuged (18 000g, 10 min at 4 °C), and the net free thiol content in the perchloric acid-soluble fraction (GSH) was determined. Samples incubated with dimedone (5 mM, 30 min at 37 °C) before GSH addition were included. Separate controls revealed that perchloric acid did not oxidize GSH. GSSG content in the neutralized supernatants was determined with NADPH (*22*). Reactions were started by the addition of glutathione reductase (0.1 U mL^{-1}) to mixtures containing NADPH (50 μM) and supernatants in phosphate buffer (0.1 M, pH 7.0, EDTA 1 mM). The concentration of GSSG was related to the loss of absorbance at 340 nm (ϵ = 6.2 mM^{-1} cm^{-1}) and validated with known amounts of GSSG. To quantify the formation of mixed HSA-glutathione disulfides, samples incubated with hydrogen peroxide followed by catalase and glutathione were subjected to gel filtration, and the thiol and protein concentrations were determined. Then, aliquots were treated with sodium borohydride (5 mM) followed by precipitation with perchloric acid. GSH content was determined by the glutathione reductase method (*23*). Briefly, NADPH (0.2 mM) was added to reaction mixtures containing DTNB (126 μM), glutathione reductase (0.1 U mL^{-1}), and supernatants containing GSH in phosphate buffer (0.1 M, pH 7.0, EDTA 1 mM). Reaction rates were determined from the slopes of the linear portions of time courses at 412 nm and related to GSH concentration using calibration curves with known amounts of GSH. Unappreciable rates were observed in controls where GSH or glutathione reductase were omitted.
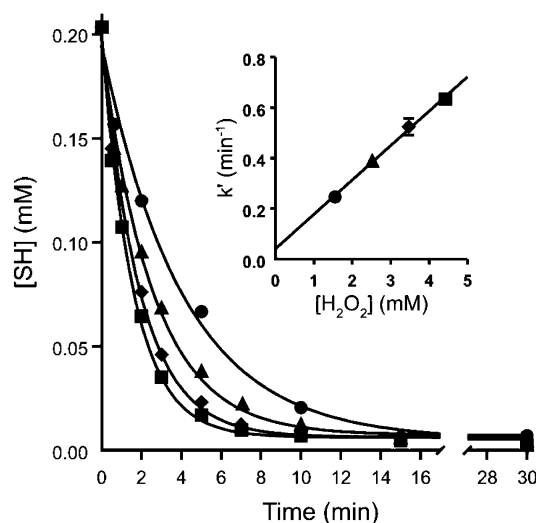

FIGURE 1: Kinetics of the reaction between hydrogen peroxide and HSA-SH. HSA (0.25 mM) was incubated with hydrogen peroxide at concentrations of 1.55 mM (circles), 2.52 mM (triangles), 3.47 mM (diamonds), and 4.42 mM (squares) in phosphate buffer (50 mM, pH 7.4, DTPA 0.1 mM) at 37 °C. Aliquots were removed at increasing time points, and the reactions were stopped with catalase (100 U mL^{-1}). The results were fitted to an exponential function to determine the pseudo-first-order rate constants (k'). (Inset) Pseudo-first-order rate constants were plotted as a function of hydrogen peroxide.

HSA Structure and Data Processing. HSA sequence and structure were obtained from the protein and structure data banks of PubMed, accession codes CAA01217 and 1BM0, respectively. Structural information was processed with Swiss-PDBViewer and Persistence of Vision Ray Tracer. Polar and nonpolar residues were defined according to Kyte and Doolittle (*24*). Chemical reaction simulations from known rate constants and initial concentrations were performed with Gepasi (*25, 26*). Data were plotted and analyzed using SlideWrite.

RESULTS

Rate Constant and Stoichiometry of the Reaction between Hydrogen Peroxide and HSA-SH. Hydrogen peroxide oxidized the thiol in HSA. In the presence of excess hydrogen peroxide, the decrease in thiol concentration fitted the exponential function [HSA-SH] = [HSA-SH]$_0$e$^{-k't}$, suggesting that the reaction is first order in thiols (Figure 1)

$$\text{HSA-SH} + \text{H}_2\text{O}_2 \xrightarrow{k} \text{products} \quad (1)$$
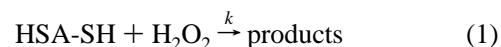
$$-\frac{d[\text{HSA-SH}]}{dt} = k[\text{HSA-SH}][\text{H}_2\text{O}_2] = k'[\text{HSA-SH}] \quad (2)$$

where k is the second-order rate constant, and k' is the pseudo-first-order rate constant, $k[\text{H}_2\text{O}_2]$. When the pseudo-first-order rate constants k' were plotted as a function of hydrogen peroxide, a linear response was obtained (Figure 1 inset), confirming that the reaction is first order in hydrogen peroxide. From the slope, a second-order rate constant of 2.26 M^{-1} s^{-1} at pH 7.4 and 37 °C was calculated. This value is comparable to that obtained via a different procedure for estimating the thiol reactivity toward hydrogen peroxide in bovine serum albumin (k = 1.14 M^{-1} s^{-1}) (*4*).

The reaction of hydrogen peroxide with HSA proceeded with a 1:1 stoichiometry, as calculated from the intercepts
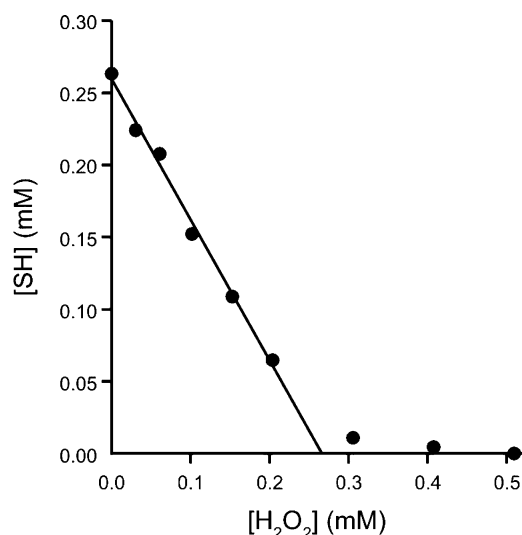
FIGURE 2: Stoichiometry of the reaction between hydrogen peroxide and HSA-SH. HSA (0.5 mM) was exposed to hydrogen peroxide (0−0.5 mM) under similar conditions as in Figure 1, and samples were assayed for thiol content at a fixed time point of 75 min.
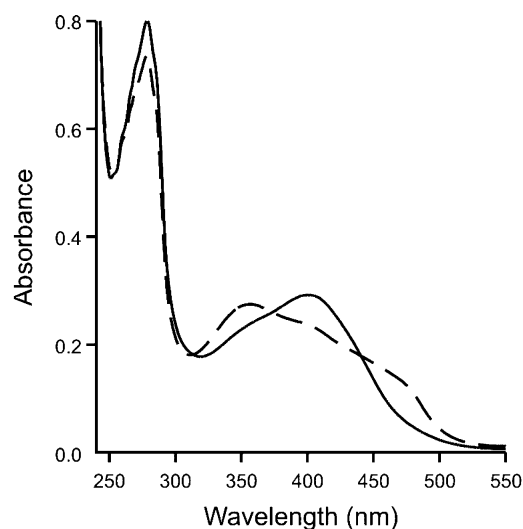

FIGURE 3: UV−vis spectra of the NBD adducts of native and hydrogen peroxide-treated HSA. HSA (0.5 mM, 0.95 SH/HSA) in phosphate buffer (0.1 M, pH 7.4, DTPA 0.1 mM), either control (solid line) or treated with 0.4 mM hydrogen peroxide for 30 min at 37 °C (broken line), was incubated with NBD-Cl for 30 min at 37 °C, followed by gel filtration to remove unreacted NBD-Cl.

of the plot of thiols remaining versus hydrogen peroxide with the axes, as well as the slope of the linear plot, which was 0.975 (Figure 2). This means that, in contrast to the reaction of low molecular weight thiols, where two thiols are oxidized for each hydrogen peroxide, only one was oxidized in HSA. The 2:1 stoichiometry for low molecular weight thiols is explained by the reaction of the thiol with one hydrogen peroxide followed by the reaction of the sulfenic acid product with a second thiol

$$RSH + H_2O_2 \rightarrow RSOH + H_2O \qquad (3)$$

$$RSOH + RSH \rightarrow RSSR + H_2O \qquad (4)$$

Thus, in the case of HSA, the observation of a 1:1 stoichiometry suggested that, instead of forming inter-molecular disulfide dimers, the thiol was oxidized beyond the disulfide state. In agreement with this, SDS−PAGE showed that exposure of HSA to hydrogen peroxide did not yield 2-mercaptoethanol-reducible dimers (data not shown), confirming that the formation of intermolecular disulfide bonds was not occurring in these conditions.

Detection of Sulfenic Acid with NBD-Cl. Although the formation of a sulfenic acid intermediate from a two-electron oxidant such as hydrogen peroxide in the presence of DTPA is likely to occur, sulfenic acid is unstable. Sulfenic acid stabilization in HSA has not been demonstrated, although its formation is suggested by arsenite reducibility of HSA oxidation products (*3, 4*). The formation of sulfenic acid has also been proposed in HSA exposed to nitric oxide under anaerobic conditions (*27*).

To detect the formation of sulfenic acid, the electrophilic reagent NBD-Cl was used, which has been previously applied to detect the formation of sulfenic acid in peroxiredoxin alkylhydroperoxide reductase exposed to hydrogen peroxide and peroxynitrite (*28, 29*) and in tyrosine phosphatase exposed to hydrogen peroxide (*30*). NBD-Cl is able to react with both thiol and sulfenic acid, forming two adducts that have different UV−vis absorption properties. The thioether adduct formed with the thiol (RS-NBD) absorbs at ∼420

nm, while the sulfoxide adduct formed with the sulfenate (RSO-NBD) absorbs at ∼350 nm (*28*). NBD-Cl can also react with tyrosyl and amine groups, particularly at alkaline pH. The absorption maxima then shift to 385 and 480 nm, respectively (*31*).

Albumin reaction with NBD-Cl yielded an absorbance spectrum with a peak at 400 nm, revealing the formation of the HSA-S-NBD adduct (Figure 3). When HSA was pre-treated with hydrogen peroxide, the 400 nm peak decreased, and a maximum at 356 nm appeared, consistent with the formation of the HSA-SO-NBD adduct. In control reactions, a slight shoulder at 356 nm was also observed, consistent with the presence of a low concentration of sulfenic acid in native HSA maintained under aerobic conditions. In hydro-gen peroxide-exposed HSA, an increase at ∼480 nm was also observed in addition to the increase in absorbance at 356 nm. This increase can also be observed in the spectra reported for tyrosine phosphatase (*30*), and its origin is unknown.

To make a rough estimate of the yield of sulfenic acid from the NBD-Cl spectral data, we assumed that the HSA-SO-NBD adduct had the same extinction coefficient as HSA-S-NBD (13 600 M^{-1} cm^{-1}; this paper and refs *28* and *30*) and thus estimated that ∼74% of the hydrogen peroxide-oxidized thiols in HSA were trapped as sulfenic acid with NBD-Cl.

As a control, the spectra of reaction mixtures containing NBD-Cl and low molecular weight thiols in different oxidation states were obtained (Figure 4). NBD-Cl alone showed a maximum at 343 nm. With GSH, the NBD-Cl peak decreased, and a new maximum appeared at 420 nm, consistent with the formation of the glutathione-*S*-NBD adduct. With cysteine, a peak was observed at 470 nm because of the formation of the *N,S*-bis-NBD derivative preceded by intramolecular S → N transfer (*32*). The observation of a maximum with HSA-SH at 400 nm (Figure 3) instead of 420 nm as for GSH may be due to the fact that the environment of the thiol in the protein could be changing
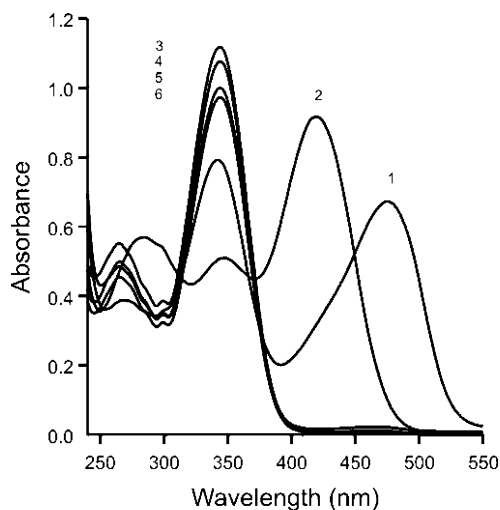
FIGURE 4: Comparative absorbance spectra of thiols in different oxidation states following incubation with NBD-Cl. Low molecular weight compounds (0.1 mM) were incubated with 0.1 mM NBD-Cl in phosphate buffer (0.1 M, pH 7.4, DTPA 0.1 mM). Cysteine (1), GSH (2), cystine (3), cysteine sulfonic acid (4), cysteic sulfinic acid (5), and no addition (6).

the spectral properties of the thiol adduct. Alternatively, it is possible that adducts with tyrosine, which absorb at 385 nm, were formed and interfered with the spectrum. No changes were detected in the spectrum of NBD-Cl with cysteine sulfinic acid, cysteine sulfonic acid, or cystine. In aggregate, these controls support that the absorbance maximum at 356 nm following HSA-SH reaction with hydrogen peroxide is due to sulfenic acid formation since no other thiol oxidation product yielded comparable results.

Trapping of Sulfenic Acid with Dimedone and Mass Spectrometry. The nucleophilic reagent dimedone does not react with reduced thiol and forms an adduct with sulfenic acid (*33*) that can be detected with mass spectrometry. Samples containing native or hydrogen peroxide-oxidized HSA were treated with dimedone and digested with trypsin after reductive alkylation with dithiothreitol and iodoacetic acid. This was done to prevent exchange reactions among cysteine-containing peptides and improve the detection of the tryptic fragment containing Cys34. ESI-tandem MS/MS analysis of proteolytic fragments revealed the Cys34-containing peptide of native HSA (residues 21−41; ALV-LIAFAQYLQQCPFEDHVK, m/z 2433.9) as the carboxy-methylated fragment (m/z 2491.9). MS/MS spectra obtained by collision-induced dissociation of $[M+3H]^{3+}$ resulted in fragmentation at the amide bonds of the parent ion (m/z 831.4) yielding type *b* or *y* ions (Figure 5A). When the protein was treated with hydrogen peroxide, a peptide with a mass increase of +138 was detected, consistent with the formation of an adduct with dimedone (m/z 2572.0). MS/MS of the $[M+3H]^{3+}$ parent ion (m/z 857.4) led to the detection of several daughter ions confirming both the identity of the fragment and the position of the dimedone modification at Cys34 (Figure 5B). As for the presence of several other ions in this spectrum, the 2271.1 peak is probably the result of y_{18} losing OH or NH_3, with the 240.1 ion possibly arising from cysteinyldimedonyl fragments. The modified peptide was not observed in native HSA, confirming that hydrogen peroxide-mediated oxidation led to the modification. From mass spectral data, it was concluded that
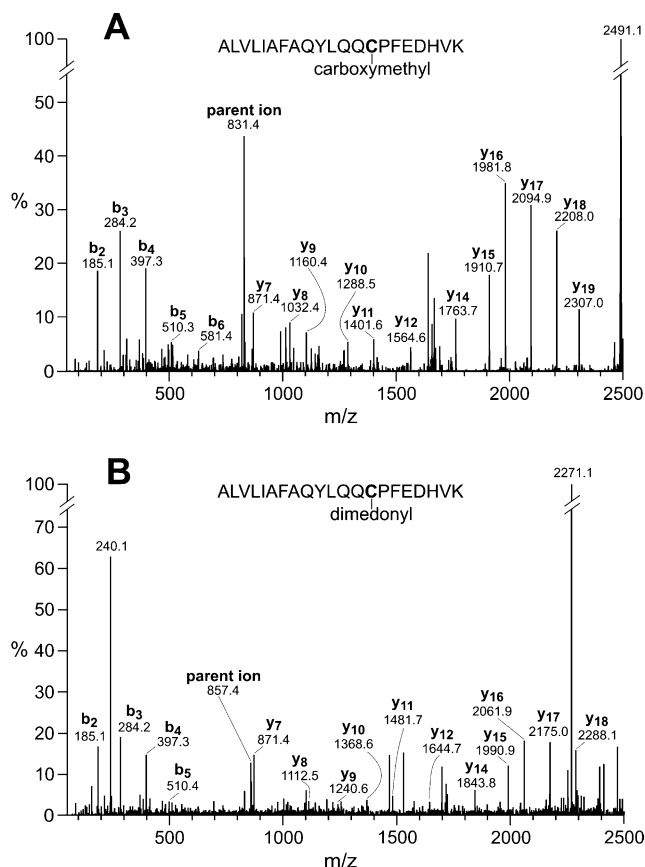

FIGURE 5: ESI-Q-TOF-MS/MS spectrum of the Cys34 tryptic fragment of dimedone-treated control and oxidized HSA. HSA (0.5 mM) was exposed to hydrogen peroxide (1 mM) in phosphate buffer (0.05 M, pH 7.4, 0.1 mM DTPA) for 30 min at 37 °C. The samples were incubated with dimedone (2.5 mM) and gel filtered. After reductive alkylation with dithiothreitol and iodoacetic acid, the samples were digested with trypsin and analyzed. (A) Control sample, parent fragment m/z 831.4 in the triply charged state. (B) Hydrogen peroxide-treated sample, parent fragment m/z 857.4 in the triply charged state. The observed *b* and *y* fragments are shown in bold.

dimedone reacted with hydrogen peroxide-treated HSA and that the site of modification was Cys34.

Reaction of Sulfenic Acid with Glutathione. Sulfenic acids react with thiols (eq 4). Indeed, exposure of GSH to hydrogen peroxide-treated HSA samples led to decreases in GSH concentration (Table 1). Dimedone was able to partially inhibit GSH oxidation by 20%, confirming HSA-SOH as an intermediate (data not shown). The extent of GSH oxidation represented 50% of HSA-SH oxidation.

To estimate sulfenic acid stability, aliquots of reaction mixtures containing hydrogen peroxide-modified HSA were withdrawn at different times. There was only a minor decrease in GSH oxidation, suggesting that more than 85% of the sulfenic acid formed in HSA remained even after 120 min (Table 1). When analyses were performed under a stream of argon, the time-dependent decrease in GSH oxidation was reduced even further (data not shown). These results indicate that oxidation of HSA-SH by hydrogen peroxide yields a relatively stable sulfenic acid derivative. The stability of the sulfenic acid was confirmed with NBD-Cl, which yielded similar spectra up to 2 h after HSA oxidation and subsequent addition of catalase (data not shown).

The reaction of sulfenic acid with thiols produces disulfides, constituting a plausible mechanism for the formation

Table 1: Reaction of Sulfenic Acid with GSH and Formation of Disulfides[a]

| time (min)	GSH oxidized (nmol)[b]	HSA-SSG (nmol)[b]	GSSG (nmol)[b]
3[c]	139 ± 5	1.67 ± 0.4	15 ± 6
30	126 ± 8	ND[d]	17 ± 6
60	129 ± 8	ND	17 ± 7
90	118 ± 13	ND	22 ± 7
120	120 ± 4	2.8 ± 0.3	20 ± 6

[a] HSA (0.5 mM) was oxidized by hydrogen peroxide (5 mM, 5 min at 37 °C) followed by the addition of catalase. Aliquots were withdrawn at different times and incubated with GSH for 30 min at 37 °C. The extents of GSH oxidation and the formation of disulfides were determined as described in Experimental Procedures. [b] The results are expressed as mean ± SD ($n = 3$). [c] The amount of thiols per HSA molecule decreased from 0.686 to 0.140 SH/HSA upon exposure to hydrogen peroxide, representing 270 nmol of oxidized HSA-SH in the 1 mL aliquots. [d] ND: not determined.

of mixed HSA disulfides and possibly accounting in part for their presence in plasma since about one-fourth of circulating HSA is present as mixed disulfides with low molecular weight thiols (*34, 35*). Further reaction of the mixed HSA disulfides with low molecular weight thiols can lead to the formation of low molecular weight disulfides. These are the predominant form of low molecular weight thiol compounds in plasma (*35*). For glutathione, the reactions involved are

$$HSA\text{-}SOH + GSH \rightarrow HSA\text{-}SSG + H_2O \qquad (5)$$

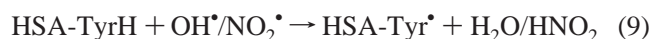$$HSA\text{-}SSG + GSH \rightleftharpoons HSA\text{-}SH + GSSG \qquad (6)$$

To confirm the formation of these disulfides, mixed HSA-glutathione disulfide and glutathione disulfide were determined after preincubation of HSA with hydrogen peroxide (Table 1). Approximately 2% of the oxidized glutathione yielded the HSA-SSG intermediate in our experimental conditions, while ~25% was recovered as GSSG. One possible explanation for this low yield is that some proportion of glutathione was oxidized beyond disulfide to higher oxidation states (e.g., sulfinic acid, sulfonic acid, thiosulfinates).

Sulfenic Acid Formation from HSA Exposed to Peroxynitrite in the Presence or Absence of Carbon Dioxide. When HSA was exposed to peroxynitrite, the thiol was oxidized (Figure 6) as expected from the fast reaction between the thiol in HSA and the peroxynitrite ($k = 3.8 \times 10^3$ M^{-1} s^{-1} at pH 7.4 and 37 °C (*5*)).

$$HSA\text{-}SH + ONOOH \rightarrow products \qquad (7)$$
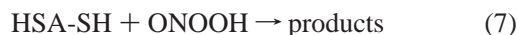
In contrast, tyrosine nitration was almost negligible under these conditions (Figure 6 inset) since most peroxynitrite reacted directly with the protein instead of homolyzing to hydroxyl and nitrogen dioxide radical intermediates primarily responsible for nitration (*5, 36, 37*).

$$ONOOH \rightarrow 0.3OH^\bullet + 0.3NO_2^\bullet + 0.7NO_3^- + 0.7H^+ \quad (8)$$

$$HSA\text{-}TyrH + OH^\bullet/NO_2^\bullet \rightarrow HSA\text{-}Tyr^\bullet + H_2O/HNO_2 \quad (9)$$

$$HSA\text{-}Tyr^\bullet + NO_2^\bullet \rightarrow HSA\text{-}TyrNO_2 \qquad (10)$$

The homolysis of peroxynitrite to hydroxyl and nitrogen dioxide radicals occurs with a relatively slow rate constant
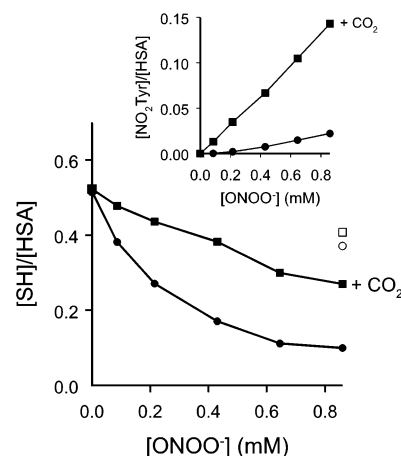

FIGURE 6: Thiol oxidation in HSA exposed to peroxynitrite. Peroxynitrite was added to HSA (0.5 mM) in phosphate buffer (0.1 M, pH 7.4, DTPA 0.1 mM), in the absence (circles) or presence (squares) of sodium bicarbonate (25 mM), for 5 min at 37 °C. (Inset) Nitrotyrosine. Results are the mean of duplicates that differed less than 10% for a representative experiment. Open symbols correspond to the reverse order of addition control, where peroxynitrite was decomposed in buffer previous to HSA addition.

of 0.9 s^{-1} at pH 7.4 and 37 °C and a 30% yield. In our experimental conditions, most peroxynitrite (81%) reacted directly with HSA instead of homolyzing to free radical products (6%) according to computer assisted calculations using the known rate constants (not shown).

In the presence of carbon dioxide, thiol oxidation was partially inhibited (Figure 6) since most peroxynitrite, instead of reacting with HSA, reacted with carbon dioxide ($k = 4.6 \times 10^4$ M^{-1} s^{-1} at pH 7.4 and 37 °C (*38, 39*)). From this, it can be calculated that more than 90% of peroxynitrite first reacted with carbon dioxide, leading to nitrogen dioxide and carbonate radicals in ~35% yield (*40−42*).

$$ONOO^- + CO_2 \rightarrow$$
$$0.35CO_3^{\bullet-} + 0.35NO_2^\bullet + 0.65NO_3^- + 0.65CO_2 \quad (11)$$
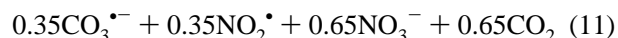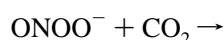
Thus, the inhibition of thiol oxidation by carbon dioxide was incomplete since secondary radical products still oxidized the thiol. Nitration of HSA was elevated 7-fold in the presence of carbon dioxide (Figure 6 inset) because of the increased formation of nitrogen dioxide in concert with the carbonate radical, which is more efficient at forming a tyrosyl radical than the hydroxyl radical formed from peroxynitrite homolysis in the absence of carbon dioxide. As for hydrogen peroxide, there was no SDS−PAGE-detectable formation of HSA dimers upon HSA exposure to peroxynitrite and peroxynitrite/CO_2 (data not shown).

In HSA exposed to peroxynitrite and peroxynitrite/CO_2, NBD-Cl addition revealed a decrease in absorbance at 400 nm and a new peak at 356 nm, consistent with the formation of sulfenic acid (Figure 7). In HSA oxidized by peroxynitrite/CO_2, the 400 nm absorbance did not decrease as much as in the absence of carbon dioxide, consistent with the limitation of thiol oxidation in the presence of carbon dioxide. Thus, NBD-Cl spectral analyses are consistent with sulfenic acid derivatives of HSA being formed upon exposure to peroxynitrite both in the presence and in the absence of carbon dioxide. In addition, peroxynitrite-treated HSA was able to oxidize glutathione, corroborating the formation of sulfenic
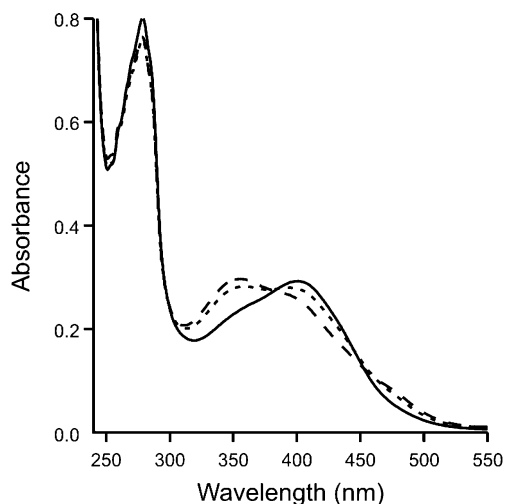
FIGURE 7: UV−vis spectra of the NBD adducts of HSA exposed to peroxynitrite and peroxynitrite/CO_2. HSA (0.5 mM), control (−) or treated with peroxynitrite (0.4 mM) in the absence (− − −) or presence (- - -) of carbon dioxide (25 mM Na-HCO$_3$/1.2 mM CO_2) for 5 min at 37 °C in phosphate buffer (0.1 M, pH 7.4, DTPA 0.1 mM), was incubated with NBD-Cl for 30 min at 37 °C, followed by gel filtration to remove unreacted NBD-Cl.

acid (data not shown). HSA treated with peroxynitrite/CO_2 also oxidized glutathione (50% as compared to samples without CO_2), in agreement with the formation of sulfenic acid in these conditions. The stability of sulfenic acid in the presence of peroxynitrite decomposition products was comparable to that of hydrogen peroxide-treated samples (data not shown).

DISCUSSION

The thiol in HSA is oxidized at relatively slow rates by hydrogen peroxide and peroxynitrite, with rate constants of 2.26 and 3.8×10^3 M^{-1} s^{-1}, respectively (5). The reactivity of the HSA Cys34 thiol is not enhanced by the protein microenvironment but rather is comparable to that of low molecular weight thiols such as cysteine ($k = 2.9$ and 4.5×10^3 M^{-1} s^{-1} for hydrogen peroxide and peroxynitrite, respectively) or GSH ($k = 0.87$ and 1.3×10^3 M^{-1} s^{-1}) (4, 43, 44). In contrast, other proteins such as peroxiredoxins, glyceraldehyde 3-phosphate dehydrogenase, creatine kinase, or tyrosine phosphatases have thiols that are several orders of magnitude more reactive (29, 45−48).

In this regard, the thiol in HSA also undergoes relatively slow thiol-disulfide exchange with the low molecular weight disulfides present in plasma. For example, there is an unappreciable rate constant for exchange of BSA with cystine and GSSG (49), and there was minimal HSA-SH oxidation when HSA was incubated with GSSG for 30 min (data not shown).

The fact that the thiol in HSA is not particularly reactive is in line with its relatively high pK_a since reactive protein thiols have unusually low pK_a values. Instead, the pK_a of HSA-SH is comparable to those of cysteine (8.36) and GSH (8.75). The pK_a of BSA-SH has been estimated to be 8.0−8.6 through ultraviolet absorption measurements (4) or reactivity with disulfides (49), while that of HSA-SH was estimated to be 8.3−8.6 through reactivity toward peroxynitrite (5).

While the Cys34 thiol of HSA is not highly reactive, this is compensated in part by the high HSA concentrations present in plasma (∼0.6 mM); thus, it is likely that HSA-SH remains an important scavenger of reactive oxygen and nitrogen species in the vascular compartment.

The fact that the stoichiometry of hydrogen peroxide oxidation was 1:1 and no 2-mercaptoethanol reducible HSA dimers were observed by SDS−PAGE shows that the formation of intermolecular disulfide dimers is not possible in HSA, most likely because of steric restrictions. The crystal structure of HSA (reproduced in Figure 8) supports this, showing Cys34 in a cleft that would preclude dimer formation. Because of its sequestration, this thiol will then more readily achieve higher oxidation states, as indicated by the NBD-Cl, dimedone, and GSH-mediated trapping of a significant amount of peroxide-induced HSA sulfenic acid. The amounts of trapped sulfenic acid were not stoichiometric, consistent with the precept that HSA thiols will also be overoxidized to sulfinic and sulfonic acids (50). Mass spectral analyses using dimedone both confirmed that a sulfenic acid derivative was formed by peroxide oxidation of HSA Cys34 and provided the definitive evidence for the formation of this intermediate in HSA.
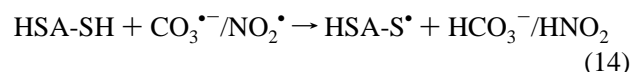
The molecular mechanisms underlying the formation of sulfenic acid from hydrogen peroxide plus DTPA, which represents a typical two-electron oxidation system, likely involves the nucleophilic attack of the thiolate anion on the peroxidic oxygens.

$$HSA\text{-}S^- + HOOH \rightarrow HSA\text{-}SOH + OH^- \quad (12)$$

The formation of sulfenic acid derivatives by peroxynitrite in the absence of carbon dioxide will involve an analogous mechanism (51).

$$HSA\text{-}S^- + ONOOH \rightarrow HSA\text{-}SOH + NO_2^- \quad (13)$$

Free radical mechanisms are not likely at the high concentrations of HSA used, with the predicted formation of free radicals shown to be minimal from computer-assisted calculations and the observation that extents of nitrotyrosine formation were low. The detection of sulfenic acid from peroxynitrite in the presence of carbon dioxide was unexpected since most peroxynitrite/CO_2 predominantly decays through free radical pathways. Thus, a free radical pathway is proposed for sulfenic acid formation induced by peroxynitrite in the presence of carbon dioxide, wherein the thiol of HSA becomes oxidized by carbonate or nitrogen dioxide radicals to thiyl radical (RS$^\bullet$). In turn, this thiyl radical can react with dioxygen, forming peroxyl radicals (RSOO$^\bullet$). These are unstable intermediates and can yield the sulfinyl radical (RSO$^\bullet$), which in turn could produce RSOH after hydrogen abstraction from adventitious reductants (AH). This proposed mechanism would thus involve the following reactions:

$$HSA\text{-}SH + CO_3^{\bullet-}/NO_2^\bullet \rightarrow HSA\text{-}S^\bullet + HCO_3^-/HNO_2$$
$$(14)$$

$$HSA\text{-}S^\bullet + O_2 \rightarrow HSA\text{-}SOO^\bullet \rightarrow HSA\text{-}SO^\bullet + [O] \quad (15)$$

$$HSA\text{-}SO^\bullet + AH \rightarrow HSA\text{-}SOH + A^\bullet \quad (16)$$
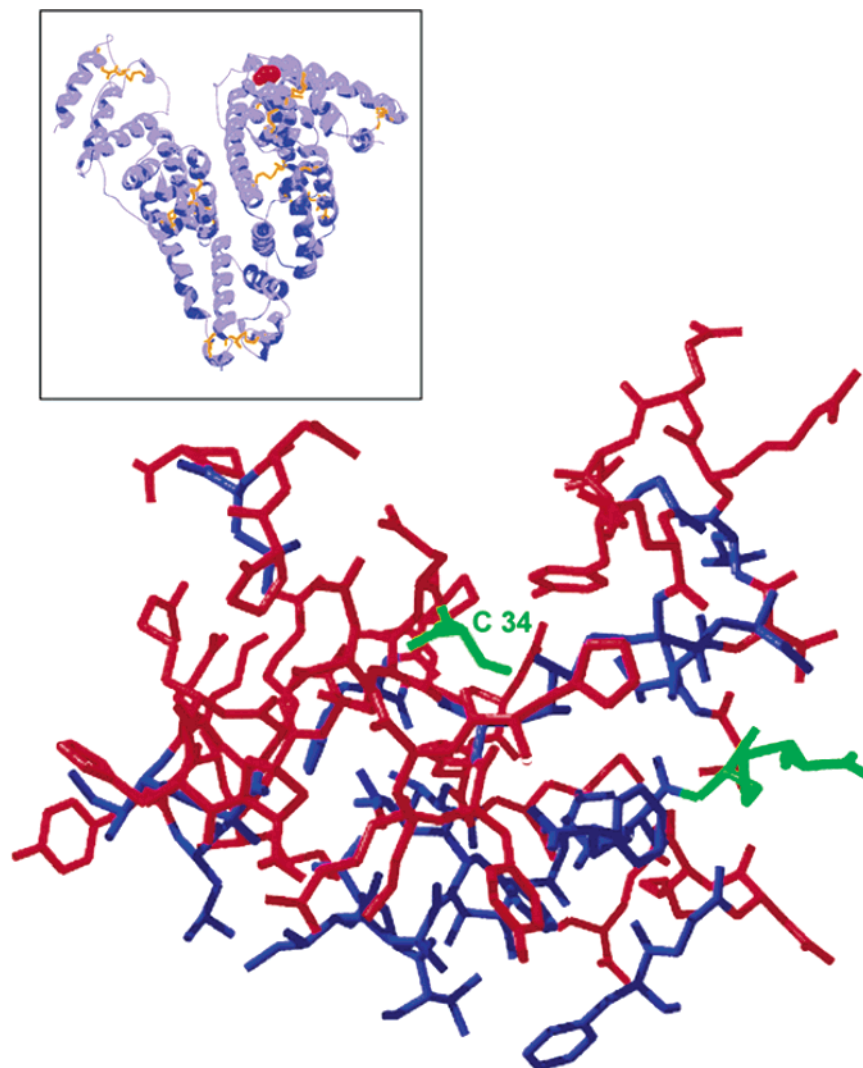
FIGURE 8: Crystal structure of the Cys34 thiol region of HSA. Shown are groups within 12 Å of Cys34. Polar residues are shown in red, and nonpolar residues are shown in blue. Cysteines are shown in green. (Inset) Heart-shape structure of HSA. The locations of the disulfide bonds are shown in orange, and Cys34 is shown in red. The amino terminus is at the right and the carboxyl terminus at the left.

In support of this proposed mechanism for RSOH formation, it is noted that carbon dioxide promotes the formation of thiyl radical from peroxynitrite reaction with low molecular weight thiols and BSA (*52, 53*). In addition, the formation of the sulfinyl radical has been detected by electron paramagnetic spectroscopy (EPR) during the oxidation of cysteine and GSH by peroxynitrite in the presence of carbon dioxide (*53*). Alternatively, it is possible that sulfenic acid formation involves a nitrothiol as an intermediate. The nitrothiol would react with water to give the sulfenic (*54*).

$$HSA\text{-}S^{\bullet} + NO_2 \rightarrow HSA\text{-}SNO_2 \qquad (17)$$

$$HSA\text{-}SNO_2 + OH^- \rightarrow HSA\text{-}SOH + NO_2^- \qquad (18)$$

In this sense, the formation of nitrothiols from peroxynitrite and GSH has been reported before (*55*).

Overall, our results provide evidence for the formation of a remarkably stable sulfenic acid in HSA. Structurally, it is likely that the microenviroment of Cys34 stabilizes this thiol oxidation state since the partially solvent-protected cleft contains no other adjacent thiol and there are several putative groups that could participate in hydrogen bonding events with

the sulfenic acid or its corresponding sulfenate (Figure 8; ref *13*).

For a protein such as HSA, whose thiol is relatively unreactive, it is remarkable that the sulfenic acid is stabilized. In this sense, it is tempting to speculate that the formation of sulfenic acid from HSA reaction with reactive oxygen and nitrogen-derived inflammatory mediators culminates in the formation of disulfides. In fact, about 25% of circulating HSA is forming mixed disulfides with cysteine (146 μM), cysteinylglycine (19.7 μM), homocysteine (7.3 μM), γ-glutamylcysteine (1.2 μM), and GSH (0.7 μM) (*34, 35*). Since these disulfides are not observed during the secretion of HSA by hepatic cells, it is likely that they are acquired in the circulation. In addition, HSA sulfenic acid could act as an intermediate in the formation of low molecular weight disulfides since, with the probable exception of glutathione, their concentration in plasma is greater than that of reduced thiols (57 μM cystine vs 9 μM reduced cysteine, 6.8 μM cysteinylglycine disulfide vs 2.6 μM reduced cysteinylglycine, 1.1 μM homocystine vs 0.17 reduced homocysteine, and 1.6 μM GSSG vs 3.4 μM reduced GSH (*35*)). Mixed HSA disulfides could also be formed by thiol-disulfide exchange of HSA-SH with cystine, GSSG, and other low

molecular weight disulfides. However, thiol-disulfide exchange is a relatively slow process for HSA (ref *49* and this paper).

On the basis of the data reported herein, it is proposed that the stable sulfenic acid formed following HSA oxidation is involved in the formation of disulfides. This could represent a protective mechanism toward reactive oxygen and nitrogen species, particularly since sulfenic acid was also observed herein to be formed through free radical pathways. Thus, the formation of a stabilized sulfenic acid in HSA could limit the oxidation of the plasma thiols to more irreversible states.

ACKNOWLEDGMENT

REFERENCES

1. Halliwell, B. (1988) *Biochem. Pharmacol. 37*, 569−71.
2. Halliwell, B., and Gutteridge, J. M. (1990) *Arch. Biochem. Biophys. 280*, 1−8.
3. Radi, R., Bush, K. M., Cosgrove, T. P., and Freeman, B. A. (1991) *Arch. Biochem. Biophys. 286*, 117−25.
4. Radi, R., Beckman, J. S., Bush, K. M., and Freeman, B. A. (1991) *J. Biol. Chem. 266*, 4244−50.
5. Alvarez, B., Ferrer-Sueta, G., Freeman, B. A., and Radi, R. (1999) *J. Biol. Chem. 274*, 842−8.
6. Hurst, R., Bao, Y., Ridley, S., and Williamson, G. (1999) *Biochem. J. 338*, 723−8.
7. Leto, S., Yiengst, M. J., and Barrows, C. H., Jr. (1970) *J. Gerontol. 25*, 4−8.
8. Era, S., Kuwata, K., Imai, H., Nakamura, K., Hayashi, T., and Sogami, M. (1995) *Biochim. Biophys. Acta 1247*, 12−6.
9. Quinlan, G. J., Margarson, M. P., Mumby, S., Evans, T. W., and Gutteridge, J. M. (1998) *Clin. Sci. (London) 95*, 459−65.
10. Janatova, J., Fuller, J. K., and Hunter, M. J. (1968) *J. Biol. Chem. 243*, 3612−22.
11. Noel, J. K., and Hunter, M. J. (1972) *J. Biol. Chem. 247*, 7391−406.
12. Claiborne, A., Miller, H., Parsonage, D., and Ross, R. P. (1993) *FASEB J. 7*, 1483−90.
13. Claiborne, A., Yeh, J. I., Mallett, T. C., Luba, J., Crane, E. J., III, Charrier, V., and Parsonage, D. (1999) *Biochemistry 38*, 15407−16.
14. Chen, R. F. (1967) *J. Biol. Chem. 242*, 173−81.
15. Bunk, D. M. (1997) *Anal. Chem. 69*, 2457−63.
16. Claiborne, A. (1985) in *Handbook of Methods for Oxygen Radical Research* (Greenwald, R. A., Ed.) pp 283−284, CRC Press, Inc., Boca Raton, FL.
17. Beckman, J. S., Beckman, T. W., Chen, J., Marshall, P. A., and Freeman, B. A. (1990) *Proc. Natl. Acad. Sci. U.S.A. 87*, 1620−4.
18. Saha, A., Goldstein, S., Cabelli, D., and Czapski, G. (1998) *Free Radical Biol. Med. 24*, 653−9.
19. Hughes, M. N., and Nicklin, H. G. (1968) *J. Chem. Soc. A 450−2*.
20. Ellman, G., and Lysko, H. (1979) *Anal. Biochem. 93*, 98−102.
21. Beckman, J. S., Ischiropoulos, H., Zhu, L., van der Woerd, M.,

Smith, C., Chen, J., Harrison, J., Martin, J. C., and Tsai, M. (1992) *Arch. Biochem. Biophys. 298*, 438−45.
22. Sies, H., and Akerboom, T. P. (1984) *Methods Enzymol. 105*, 445−51.
23. Tietze, F. (1969) *Anal. Biochem. 27*, 502−22.
24. Kyte, J., and Doolittle, R. F. (1982) *J. Mol. Biol. 157*, 105−32.
25. Mendes, P. (1993) *Comput. Appl. Biosci. 9*, 563−71.
26. Mendes, P. (1997) *Trends Biochem. Sci. 22*, 361−3.
27. DeMaster, E. G., Quast, B. J., Redfern, B., and Nagasawa, H. T. (1995) *Biochemistry 34*, 11494−9.
28. Ellis, H. R., and Poole, L. B. (1997) *Biochemistry 36*, 15013−8.
29. Bryk, R., Griffin, P., and Nathan, C. (2000) *Nature 407*, 211−5.
30. Denu, J. M., and Tanner, K. G. (1998) *Biochemistry 37*, 5633−42.
31. Aboderin, A. A., and Boedefeld, E. (1976) *Biochim. Biophys. Acta 420*, 177−86.
32. Birkett, D. J., Price, N. C., Radda, G. K., and Salmon, A. G. (1970) *FEBS Lett. 6*, 346−8.
33. Benitez, L. V., and Allison, W. S. (1974) *J. Biol. Chem. 249*, 6234−43.
34. Andersson, L. O. (1966) *Biochim. Biophys. Acta 117*, 115−33.
35. Andersson, A., Isaksson, A., Brattstrom, L., and Hultberg, B. (1993) *Clin. Chem. 39*, 1590−7.
36. Radi, R., Denicola, A., Alvarez, B., Ferrer-Sueta, G., and Rubbo, H. (2000) in *Nitric Oxide* (Ignarro, L., Ed.) pp 57−82, Academic Press, San Diego.
37. Trujillo, M., Naviliat, M., Alvarez, M. N., Peluffo, G., and Radi, R. (2000) *Analusis 28*, 518−527.
38. Lymar, S. V., and Hurst, J. K. (1995) *J. Am. Chem. Soc. 117*, 8867−8.
39. Denicola, A., Freeman, B. A., Trujillo, M., and Radi, R. (1996) *Arch. Biochem. Biophys. 333*, 49−58.
40. Goldstein, S., and Czapski, G. (1997) *Inorg. Chem. 36*, 5113−7.
41. Lymar, S. V., and Hurst, J. K. (1998) *Inorg. Chem. 37*, 294−301.
42. Bonini, M. G., Radi, R., Ferrer-Sueta, G., Ferreira, A. M. D. C., and Augusto, O. (1999) *J. Biol. Chem. 274*, 10802−10806.
43. Winterbourn, C. C., and Metodiewa, D. (1999) *Free Radical Biol. Med. 27*, 322−8.
44. Koppenol, W. H., Moreno, J. J., Pryor, W. A., Ischiropoulos, H., and Beckman, J. S. (1992) *Chem. Res. Toxicol. 5*, 834−42.
45. Hofmann, B., Hecht, H. J., and Flohe, L. (2002) *Biol. Chem. 383*, 347−64.
46. Souza, J. M., and Radi, R. (1998) *Arch. Biochem. Biophys. 360*, 187−94.
47. Konorev, E. A., Hogg, N., and Kalyanaraman, B. (1998) *FEBS Lett. 427*, 171−4.
48. Takakura, K., Beckman, J. S., MacMillan-Crow, L. A., and Crow, J. P. (1999) *Arch. Biochem. Biophys. 369*, 197−207.
49. Wilson, J. M., Wu, D., Motiu-DeGrood, R., and Hupe, D. J. (1980) *J. Am. Chem. Soc. 102*, 359−63.
50. Finch, J. W., Crouch, R. K., Knapp, D. R., and Schey, K. L. (1993) *Arch. Biochem. Biophys. 305*, 595−9.
51. Trujillo, M., and Radi, R. (2002) *Arch. Biochem. Biophys. 397*, 91−8.
52. Gatti, R. M., Radi, R., and Augusto, O. (1994) *FEBS Lett. 348*, 287−90.
53. Bonini, M. G., and Augusto, O. (2001) *J. Biol. Chem. 276*, 9749−54.
54. Torchinsky, Y. M. (1981) *Sulfur in Proteins*, Pergamon Press Ltd., Oxford.
55. Balazy, M., Kaminski, P. M., Mao, K., Tan, J., and Wolin, M. S. (1998) *J. Biol. Chem. 273*, 32009−15.